Solar Energy Materials and Solar Cells 172 (2017) 238–243

Contents lists available at ScienceDirect

Solar Energy Materials and Solar Cells

journal homepage: www.elsevier.com/locate/solmat

Photovoltaic characterisation of GaAsBi/GaAs multiple quantum well devices

R.D. Richards[a,*], A. Mellor[b], F. Harun[a], J.S. Cheong[a], N.P. Hylton[b], T. Wilson[b], T. Thomas[b], J.S. Roberts[a], N.J. Ekins-Daukes[b], J.P.R. David[a]

[a] University of Sheffield, Sheffield, South Yorkshire, S1 3JD, UK
[b] Imperial College London, London SW7 2AZ, UK

ARTICLE INFO

Keywords:
GaAsBi
MQWs
Multijunction
IQE
InGaAs

ABSTRACT

A series of strained GaAsBi/GaAs multiple quantum well diodes are characterised to assess the potential of GaAsBi for photovoltaic applications. The devices are compared with strained and strain-balanced InGaAs based devices.

The dark currents of the GaAsBi based devices are around 20 times higher than those of the InGaAs based devices. The GaAsBi devices that have undergone significant strain relaxation have dark currents that are a further 10–20 times higher.

Quantum efficiency measurements show the GaAsBi devices have a lower energy absorption edge and stronger absorption than the strained InGaAs devices. These measurements also indicate incomplete carrier extraction from the GaAsBi based devices at short circuit, despite the devices having a relatively low background doping. This is attributed to hole trapping within the quantum wells, due to the large valence band offset of GaAsBi.

1. Introduction

The current world record solar cell efficiency is held by a multi-junction device [1]. Multi-junction devices absorb different portions of the solar spectrum in different sub-cells, minimising the below-band gap and thermalisation losses in the device [2]. Maximising the efficiency of a multi-junction solar cell requires the band gaps of the sub-cells to be well optimised, balancing the current produced by each sub-cell. Finding lattice matched materials at the appropriate band gaps has proven very difficult, necessitating techniques such as metamorphic growth and wafer bonding [3]. Multiple quantum well (MQW) systems have also been developed to overcome this issue and have yielded very high efficiencies in commercially available devices [4]. InGaAs based MQWs have been used in GaAs sub-cells to extend their absorption edge; however, strain has been a problem with this approach and even with strain balancing, the critical thickness of each quantum well (QW) has historically limited the absorption of these devices to ~ 1.3 eV [4]. More recently, interlayered QW designs have been produced that absorb at longer wavelengths [5–8]; these designs incorporate layers of intermediate lattice constant and band gap between the QWs and barriers. This has enabled InGaAs/GaAsP MQW absorption to extend to 1.13 eV [8]. The intermediate layers have two effects: they reduce the impact of the abrupt lattice constant change on the crystal quality [7,9]; they also reduce the quantum confinement energy of the QWs and aid thermionic carrier escape [5,6]. Theoretically, an infinite number of QWs can be stacked without lattice relaxation, provided that the average strain of the QWs and barriers integrates to zero. However, maximising the long wavelength absorption of the MQW stack necessarily means maximising the In content of the QWs. In order to maintain strain balance and a reasonable total MQW thickness, this also requires a large P content of the barriers. The resulting large lattice mismatch interface between each QW and barrier acts as a potential seeding point for dislocations and many-period MQWs often suffer from significant lattice relaxation. The incorporation of GaAs interlayers reduces the mismatch at each interface and allows thicker MQW stacks to be grown without significant relaxation [7,9]. The interlayers also impact on the carrier confinement in the QW. Adding a GaAs interlayer between an InGaAs QW and a GaAsP barrier staggers the change in potential between the QW and barrier, reducing the quantum confinement. This also combines with the potential gradient due to the

---

* Corresponding author.
E-mail addresses: R.Richards@sheffield.ac.uk (R.D. Richards), a.mellor@imperial.ac.uk (A. Mellor), fharun1@sheffield.ac.uk (F. Harun), j.s.cheong@sheffield.ac.uk (J.S. Cheong), n.hylton@imperial.ac.uk (N.P. Hylton), t.wilson14@imperial.ac.uk (T. Wilson), tomos.thomas08@imperial.ac.uk (T. Thomas), j.s.roberts@sheffield.ac.uk (J.S. Roberts), n.ekins-daukes@imperial.ac.uk (N.J. Ekins-Daukes), j.p.david@sheffield.ac.uk (J.P.R. David).

http://dx.doi.org/10.1016/j.solmat.2017.07.029
Received 10 March 2017; Received in revised form 21 June 2017; Accepted 20 July 2017

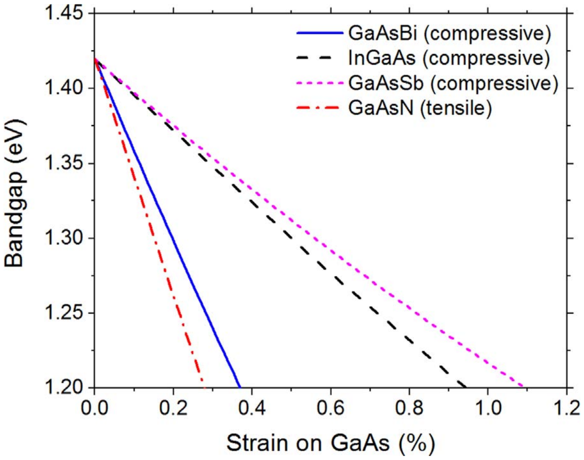

Fig. 1. Band gap vs strain for several III-V ternary alloys on GaAs over a range of compositions. The type of strain for each material is listed in the legend. The band gaps are calculated for free standing material and the strain is calculated for the same material compositions, grown pseudomorphically on GaAs. While the curves are not physically meaningful — they do not account for the effect of strain on the band gaps — they are indicative of the band engineering potential of each alloy. Data taken from [11–14].

built-in electric field to reduce the energy required to thermionically escape from the QW [5,6]. This effect may prove important, as recent work on GaInAsN — which produces large conduction band offsets on GaAs — has demonstrated electron trapping in MQW layers [10].

GaAsBi is a relatively recent material system that may be an alternative to InGaAs. The incorporation of Bi reduces the band gap of GaAs by ~ 75 meV/% Bi [11] (~ 620 meV/% strain on GaAs); which is significantly larger than the ~ 15 meV/% In [12] (240 meV/% strain on GaAs) reduction with the incorporation of In. The band gap reductions per unit strain for several III-V materials on GaAs are shown in Fig. 1.

As GaAsBi and InGaAs have approximately the same critical thickness [15], a greater range of band gaps is afforded by GaAsBi than by InGaAs while maintaining pseudomorphic material. This enhanced band engineering capability has driven a dramatic development in GaAsBi growth [16–18], with several important technological applications for the material system identified, including solar cells [19,20], lasers [21,22], spintronics [23] and detectors [24]. By applying this material system to photovoltaics, it is envisioned that the enhanced flexibility in band engineering will accelerate the development of multi-junction photovoltaics in the current bid to exceed 50% efficiency [25].

GaAsBi MQW systems have been studied for a number of years [26–28]. It has been shown that they can be subject to the same homogeneity issues as GaAsBi bulk structures [29–31]. These homogeneity issues cause the first QW in a series to be either more Bi rich or more Bi poor than the other QWs, similar to the bulk GaAsBi system [32]; this is probably caused by the chemisorbed Bi layer mediated growth mechanism of GaAsBi [33]. It has been shown, however, that careful control over the growth conditions can mitigate this effect [29,31]. The growth of GaAsBi has now progressed to the point where a GaAsBi MQW system can provide sufficient gain to realise an electrically pumped laser with emission beyond 1 μm [34]. While GaAsBi MQWs have demonstrated lasing capabilities, the absorption and photovoltaic properties of these systems have received very little attention.

In this work, a series of strained GaAsBi/GaAs MQW devices (collectively referred to as "the GaAsBi devices" henceforth) are characterised to assess their potential as solar cells. It is important that the characteristics of the strained GaAsBi system are understood before introducing strain balancing. The results are put into context by comparison with two InGaAs based MQW devices: the strained 10 period $In_{0.16}Ga_{0.84}As$/GaAs device reported by Barnes et al. [35] (henceforth referred to as "R1"); the strain-balanced 35 period interlayered InGaAs/GaAsP device reported by Toprasertpong et al. [8] (henceforth referred to as "R2").

2. Material and methods

A systematic series of GaAsBi/GaAs MQW p-i-n devices was grown by molecular beam epitaxy (MBE). The devices were grown on (100) GaAs n-type substrates and are designed as follows: 200 nm n-type GaAs buffer; 200 nm n-type $Al_{0.3}Ga_{0.6}As$ cladding; 620 nm undoped GaAsBi/GaAs MQW; 600 nm p-type $Al_{0.3}Ga_{0.6}As$ cladding; 10 nm p+ GaAs cap. The i-regions contained different numbers of evenly spaced, nominally 8 nm thick, GaAsBi QWs with GaAs barriers of the requisite thickness to maintain the total i-region thickness. The Bi content of the wells is difficult to estimate; transmission electron micrographs show that they are thinner than the nominal 8 nm and do not have abrupt interfaces [33]. As such it is very difficult to produce an accurate, meaningful X-ray diffraction fitting model of the system and calculations of the quantum confinement cannot assume "square" QWs. If one assumes "square" QWs in these devices then Bi contents of around 4.5% are estimated throughout the series [15]. In reality, the non-uniform nature of the QWs suggests that the peak Bi content is probably closer to 5%. It is possible that the graded Bi contents in these layers may alleviate the impact of the abrupt QW/barrier lattice constant change on the material quality. This may mean that careful optimisation of the growth protocol could potentially remove the need for interlayers in GaAsBi based MQW solar cells. The details of the general growth methodology [36] and the specific protocol used to grow these devices [15] have been discussed elsewhere. The device structure and details of the nominal i-region designs are shown in Fig. 2a. For clarity, the designs of the R1 and R2 are also shown in Fig. 2.

Circular mesa diodes of several radii up to 200 μm were fabricated by using standard photolithography techniques and wet etching. The back n-type contact was made using In/Ge/Au and the top p-type contact was made using Au/Zn/Au. The top contacts were annular to allow optical access to the device.

External quantum efficiency (EQE) and reflectance spectra were measured using a combination of xenon and halogen lamps coupled to a Bentham Instruments monochromator. The monochromatic light was then delivered via a 600 μm core optical fibre to a custom-built microscope system, which illuminated a small (150 × 150 μm) area. The EQEs were calibrated by measuring the incident spectrum using calibrated Si and Ge detectors. For the reflectance (R) measurement, the reflected light was measured using calibrated Si and Ge detectors and the device reflectance extracted from the raw data using corresponding measurements of a reference mirror. Internal quantum efficiency (IQE) is calculated as $IQE = EQE / (1 - R)$

Light current-voltage curves were measured under a close-matched AM1.5 spectrum ($1000\ Wm^{-2}$) using a TS-Space Systems solar simulator (Unisim). The solar simulator is dual source with a metal halide source covering the UV–Vis portion of the spectrum and a quartz halogen lamp covering the Vis-IR. The effective spectral range is 250–1800 nm. The spectrum was calibrated using a spectroradiometer. The incident light was filtered with a 900 nm long pass filter to simulate operation under an $In_{0.01}Ga_{0.99}As$ subcell in a multi-junction solar cell.

3. Results and discussion

3.1. I-V

The dark I-V curves from the GaAsBi devices are shown in Fig. 3, alongside the curves from R1 and R2. The I-V characterisation was performed on several diodes of different mesa area for each of the GaAsBi devices. The measured current densities were consistent throughout the measurements, indicating that bulk — rather than surface — conduction was taking place. All of the GaAsBi devices show good rectifying characteristics, with ideality factors between 1 and 2, although at high bias QW54 shows a non-exponential increase of